ACS APPLIED POLYMER MATERIALS

pubs.acs.org/acsapm Article

Tunable Electromagnetic Interference Shielding Properties of Binary Thermoplastic Composites Prepared by Reactive Microencapsulation

Filipa M. Oliveira, Luís Martins, Nadya V. Dencheva, Tiberio A. Ezquerra, and Zlatan Z. Denchev*

Cite This: ACS Appl. Polym. Mater. 2022, 4, 3482−3490 Read Online

ACCESS | Metrics & More | Article Recommendations | Supporting Information

ABSTRACT: Thermoplastic composites integrating carbon nanotubes (CNT) and micron-sized metal particles dispersed in polymer matrices can address emerging multifunctional needs, e.g., good electrical conductivity and electromagnetic interference (EMI) shielding combined with easy processing and affordable costs. Herein, an approach based on reactive microencapsulation is reported to prepare polyamide 6 (PA6)-based composites comprising binary loads of CNT and Al, Cu, or Fe particles. The microencapsulation is performed by activated anionic polymerization of ε-caprolactam in solution, in the presence of the metal/CNT loads. The resulting hybrid microparticles are compression-molded into plates containing effective metal/CNT loads in the range of 12−17 wt %. Among the materials synthesized, the one containing Al/CNT binary load (3:7 wt %) displays the highest EMI shielding effectiveness (SE) of 43.5 dB at 12 GHz, with a 2 mm thickness and an electrical conductivity σ_{dc} of 6.61 × 10^{-3} S/cm. A synergetic effect is observed in all of the metal/CNT PA6 samples in terms of both σ_{dc} and SE increase. Evidently, the presence of metal particles well dispersed in the conductive CNT network contributes to the mobility of the carriers and thus to the effective attenuation of the electromagnetic waves. Therefore, the binary composites of this study can be efficient thermoplastic EMI shielding materials.

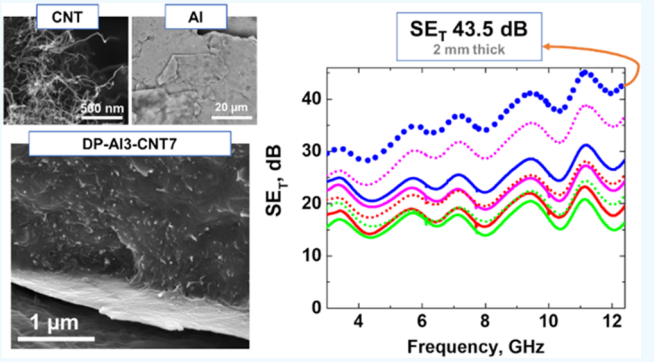

KEYWORDS: *thermoplastic composites, electromagnetic interference (EMI) shielding, electrical conductivity, polyamide 6, microencapsulation strategy*

1. INTRODUCTION

Any electric circuit is susceptible to electromagnetic interference (EMI) originating from natural sources (lightning, solar flares, etc.) or from manmade devices that can seriously upset its proper work or cause loss of stored data.[1] Moreover, anthropogenic EMI pollution can also affect biological processes, including human health.[2] These major issues have stimulated intensive studies on the nature of EMI and the development of different materials with EMI shielding or attenuation properties. Electrical and electronic devices, communication systems, scientific electronics, military and defense equipment, home appliances, and medical diagnostic equipment are examples in which materials with EMI shielding properties are required.[3−6]

The EMI shielding effectiveness (SE) can be achieved through different loss mechanisms, namely, reflection (SE_R), absorption (SE_A), and multiple reflections (SE_M).[3] Conducting metals, such as Al, Ag, Fe, and Cu, were initially broadly used as reflecting EMI shielding materials. However, high density, poor mechanical flexibility, insufficient resistance to chemicals, and costly processing caused major restrictions in the use of sole metal EMI shielding materials. Moreover, it is of practical importance to develop absorption-dominated EMI shields so as to avoid secondary pollution by reflected electromagnetic waves.[7,8] Because of these reasons, sole metal EMI shielding materials are being replaced by flexible hybrid shields based on either intrinsically conducting polymers[9,10] or conductive polymer composites (CPC).[11,12] In the latter case, insulating polymers are modified with conducting fillers with high dielectric constant (ZnO, TiO_2, $BaTiO_3$) or high magnetic permeability values ($Fe(CO)_5$, Ni, Co, Fe_2O_3), thus reaching SE values of up to 45 dB, predominantly by absorption mechanism.[13,14] Most of the electrically conductive fillers used in CPC are carbon allotropes: carbon nanotubes (CNT), expanded graphite, graphene and derivatives, or carbon black (CB).[14] The reason for this extended use is the good electrical

Received: January 13, 2022
Accepted: March 22, 2022
Published: March 31, 2022

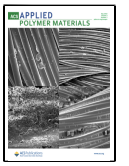

https://doi.org/10.1021/acsapm.2c00084
ACS Appl. Polym. Mater. 2022, 4, 3482−3490

conductivity of the hybrids containing carbonaceous fillers and the ability of the latter to achieve it at low percolation thresholds through the formation of a conductive interconnected network.[15]

As regards the insulating polymer matrices for EMI shielding materials from CPC, a number of thermoplastics have been tried:[14] polyolefins (mostly polyethylene and polypropylene), poly(vinylidene fluoride), polyurethanes, polyacrylates, polysiloxanes, polycarbonates, some copolymers as ABS, among others. The review of Ganguly et al.[16] reflects the state of the art in the area of EMI shielding polymer composites until 2018. More recent works disclose certain carbonaceous filled copolymers[17,18] or wood-plastic composites[19] as potential EMI shields.

Recently, there has been growing interest in CPC for EMI shielding purposes based on polyamide 6 (PA6). Thus, Duan et al.[20] disclosed PA6/expanded graphite CPC obtained by mechanical mixing and subsequent compression molding. This material displayed an effective SE of 25 dB at 10 GHz and 2.3 vol % content of the carbon allotrope, and the sample thickness is 2 mm. In a previous work of Yoo et al.,[21] Ni-coated carbon fibers embedded in a PA6 matrix as a primary filler and certain amounts of secondary fillers such as TiO_2, multiwalled CNT, or CB were employed to prepare by melt processing EMI shielding materials with relatively high SE values of 51−53 dB measured at 1 GHz, using 15 wt % of the primary and up to 3 wt % of the secondary filler. PA6/CB porous CPC composite was prepared by Cai et al.[7] by solution casting reaching SE values of 33−37 dB measured in the 8−12 GHz frequency range at 50 wt % of the CB filler. Furthermore, a PA6-graphene filament with 9 vol % of filler prepared for additive manufacturing[22] had a total SE value of 11−16 dB (sample thickness of 1 mm) in the range of 8−12 MHz. Jang et al.[23] reported the preparation of multiwalled CNT wrapped in PA6 by means of melt anionic polymerization of caprolactam. The PA6/CNT masterbatch so produced was used to prepare ABS-based composites with electrical conductivity of 0.30−2.2 S/cm claimed by the authors to be useful for EMI shielding.

So far, the CPC composites for EMI shielding purposes have been prepared exclusively by melt-processing techniques, such as extrusion or injection molding. These traditional methods need relatively high processing temperatures, most frequently with an application of more than one melting/recrystallization cycle. This creates a high possibility of material degradation due to shear forces and the temperatures applied. Poor dispersion of particulate or fibrous loads with subsequent aggregation is also a major disadvantage of melt-processing methods.[24,25] In addition, melt-blending may be complicated with elevated amounts of fillers.[26]

An alternative to overcome the limitations of conventional melt processing would be to synthesize the polymer matrix by *in situ* reactive microencapsulation, wrapping in a polymer shell one or several filler particles. PA6 is one of the few industrial thermoplastics that can be synthesized by polymerization in solution. This process allows the reactive encapsulation of the fillers′ particles in a PA6 shell thus forming micron-sized hybrid PA6-based powders. The latter can be compression-molded to composite materials containing relatively high amounts of one or more payloads. Such an approach reported previously by Dencheva et al.[27] is based on a one-pot solution/precipitation activated anionic ring-opening polymerization (AAROP) of ε-caprolactam (ECL) in the presence of different fillers, with subsequent transformation of the hybrid PA6 microparticles thus prepared into thermoplastic composite plates by compression molding. A number of composite materials were obtained by this fast and simple method comprising metal,[28] carbonaceous,[29] or mixed[30] loads, being finely dispersed within the thermoplastic PA6 matrix. None of these hybrid composites materials obtained via micro-encapsulation were ever tried as EMI shields. This inspired the present study in which microparticles (MP) comprising binary loads of multiwalled CNT and a metal filler (Al, Cu, or Fe) were prepared by AAROP and compression-molded into composite plates. Their electrical conductivity and EMI shielding properties were studied as a function of sample composition and thickness.

2. EXPERIMENTAL SECTION

2.1. Materials. The ECL monomer with reduced moisture content for AAROP (AP-Nylon caprolactam) was delivered from Brüggemann Chemical, Germany. Before use, it was dried under vacuum at 60 °C. As an activator of the AAROP of ECL, Brüggolen C20 from Brüggemann Chemical (Germany) was employed containing, according to the manufacturer, 80 wt % of aliphatic diisocyanate blocked in CL. The polymerization initiator sodium dicaprolactamato-bis-(2-methoxyethoxo)-aluminate (Dilactamate, DL) was supplied by Katchem (Czech Republic) and used without further treatment. The multiwalled CNT (≥98% of carbon content) with an outer diameter of ca. 10 nm and 3−6 μm length were purchased from Sigma-Aldrich/Merck. The powders of Cu (>99.5%, grain size <40 μm) and Al (>93%, grain size <100 μm) were supplied by Sigma-Aldrich/Merck. The soft, noninsulated Fe powder (>99.5%, average grain size 3−5 μm) was kindly donated by the BASF Group, Germany. The toluene and methanol are all "puriss" grades purchased from Sigma-Aldrich/Merck. All chemical reagents, solvents, and payloads were used as received.

2.2. Sample Preparation. The loaded PA6 microparticles were produced by solution-precipitation AAROP of ECL performed as described in detail in previous works.[27,30] In a typical polymerization, 0.5 mol of ECL, desired amounts of CNT, and metal loads (altogether up to 10 wt % in respect to ECL) were added to 100 mL of 1:1 toluene/xylene mixture while stirring. After sonication for 10 min and refluxing for another 10 min, 3 mol % DL and 1.5 mol % C20 were added at once. The polymerization time was 2 h, maintaining the temperature in the 125−135 °C range, at a constant stirring rate of ca. 800 rpm. The binary loaded metal/CNT microparticles (DM samples) formed as fine dark powders with a metallic luster were separated from the reaction mixture by hot vacuum filtration, washed several times with methanol, and dried at 80 °C. Neat PA6 particles with no load and MP with single metal or CNT loads (M-samples) were synthesized as references used in various characterization techniques. Table 1 displays samples' designation and composition of the particulate samples produced by AAROP.

The loaded MP samples were subsequently subjected to hot compression molding (CM) in a 25-ton Moore hydraulic press with hot mold (U.K.) to obtain single and binary loaded PA6 hybrid plates designated as P and DP samples, respectively. Two sets of samples for each composition with different dimensions were prepared, namely, 70 × 70 × 2 mm^3 and 85 × 75 × 1 mm^3 applying a pressure of about 5 MPa for 6−8 min at 230 °C. Then, the molded plates were cooled down to 60 °C and demolded. Figure 1 shows the visual aspect of some of the prepared samples.

2.3. Characterization and Measurements. Scanning electron microscopy (SEM) analysis was performed in a NanoSEM-200 apparatus of FEI Nova (Hillsboro) using mixed secondary electron/back-scattered electron in-lens detection. The composite plates were cryo-fractured, and the sections obtained were sputter-coated with a gold−palladium (Au−Pd) alloy, 80−20 wt %, with a thickness of about 8 nm using a 208 HR equipment of Cressington Scientific Instruments (Watford, U.K.) with high-resolution thickness control. The neat loads were analyzed as received.

https://doi.org/10.1021/acsapm.2c00084
ACS Appl. Polym. Mater. 2022, 4, 3482−3490

Table 1. Designation, Composition, and Polymerization Yields for M and DM Samples[a]

sample designation	load, wt %[b]	composition, vol %[c] metal	CNT	PA6	MP yield, wt %[d]	real load, wt %[e]
M-PA6		0	0	100	56.2	0
M-Al5	5	4.18	0	95.8	45.9	9.4
M-Cu5	5	1.33	0	98.7	42.4	9.6
M-Fe5	5	1.06	0	98.9	45.3	7.0
M-CNT3	3	0	2.65	97.4	54.6	4.9
M-CNT5	5	0	4.45	95.6	53.2	8.2
M-CNT7	7	0	6.72	93.3	52.3	12.1
DM-Al3-CNT7	3 + 7	1.96	5.71	92.3	61.0	14.4
DM-Al5-CNT5	5 + 5	3.84	4.80	91.4	50.4	16.7
DM-Al7-CNT3	7 + 3	4.68	2.51	92.8	58.9	14.7
DM-Cu5-CNT5	5 + 5	1.03	4.29	94.7	51.8	14.8
DM-Fe5-CNT5	5 + 5	0.93	3.38	95.7	63.0	11.9

[a]In the sample designations, the letter M stands for "microparticles" and DM stands for "dually loaded microparticles". [b]Percentage based on the weight of the ECL monomer in the starting AAROP mixture. [c]Represents the relation between the volumes of metal, CNT, and PA6 in the respective MP. [d]ECL conversion yield with respect to the sum of the ECL and filler weight. [e]Determined by TGA according to eq 1.

For the characterization of the particulate M and DM samples, thermogravimetric analysis (TGA) was also used to determine their effective real load (RL). A Q500 TGA equipment (TA Instruments) was employed, heating the samples from 40 to 600 °C at 10 °C/min in an N_2 atmosphere. The typical sample weights were in the 10−20 mg range. The RL value in MP was calculated according to eq 1

$$\mathrm{RL}(\%) = R_f - R_{PA6} \tag{1}$$

where R_{PA6} is the carbonized residue at 600 °C of empty PA6 MP and R_f represents the carbonized residue of the respective loaded MP measured by TGA.

The electrical conductivity, σ_{dc}, of the PA6-based composite plates (P and DP samples) was determined by a system for broadband dielectric spectroscopy (Novocontrol, Germany) supplied with an Alpha modular dielectric interface. Measurements as a function of frequency were performed at 20 °C in a frequency range from 10^{-2} to 10^7 Hz. The electrical conductivity was derived from the complex permittivity $\varepsilon^* = \varepsilon' - i\varepsilon''$, where ε' and ε'' are the real and imaginary parts of the complex permittivity, according to $\sigma(F) = \varepsilon_0 2\pi F\varepsilon''$, wherein ε_0 is the vacuum permittivity.[31] For the conductive samples, the values of the DC electrical conductivity σ_{dc} were determined from the frequency-dependent $\sigma(F)$ at low frequencies as previously described.[32,33] In the case of the nonconductive samples, the reference DC electrical conductivity values were taken at a frequency of 0.1 Hz.

The measurements were performed with P and DP plates with sputtered Au electrodes (20 mm in diameter) deposited on both surfaces.

The EMI shielding characterization of the PA6-based hybrid P and DP plates was performed at room temperature using the transmission coaxial line method (Figure 2). The measurements were executed as a function of frequency, f, over a frequency range of 3−12.4 GHz employing an N5242A PNA-X Network Analyzer (Agilent Technologies). Figure 2a displays a scheme of the apparatus. A flanged coaxial line sample holder was used connected to the vector network analyzer (VNA) by coaxial cables and connectors with 50 Ω characteristic impedance and 10 dB attenuators fixed on each end of the sample holder. A reference and load specimens with the same thickness (1 or 2 mm) were used for each composite (Figure 2b). Such specimens were cut using a laser cutting machine LightCut 6090 (G-Weike, China). The reference specimen has a 60 mm outer diameter, a 23 mm inner diameter, and it is still composed of a disk with a 10 mm diameter that matches with the internal conductor of the sample holder. The load specimen has 60 mm in diameter.

The overall SE was determined by measuring the ratio of the incident to the transmitted electric field with both reference E_R and load E_L specimens according to

$$\mathrm{SE(dB)} = 20\log_{10}\left(\frac{E_R}{E_L}\right) = \mathrm{SE_R} + \mathrm{SE_A} + \mathrm{SE_M} \tag{2}$$

wherein the shielding by reflection, SE_R, and the shielding by absorption, SE_A, were determined using the following equations[6,7,20,22]

$$\mathrm{SE_R(dB)} = -10\log_{10}(1-R) \tag{3}$$

$$\mathrm{SE_A(dB)} = -10\log_{10}\left(\frac{T}{1-R}\right) \tag{4}$$

Whenever $SE_A \gg 10$ dB, SE_M was neglected. The reflection and transmission coefficients R and T were directly determined as

$$R = |S_{11}|^2 = |S_{22}|^2 \tag{5}$$

$$T = |S_{12}|^2 = |S_{21}|^2 \tag{6}$$

Here, S represents the scattering parameters (S-parameters) through the coaxial transmission line, in which the transmission/reflection waves are collected in both directions, as sketched in Figure 2c. Hence, the total EMI SE (SE_T) was calculated as

$$\mathrm{SE_T(dB)} = \mathrm{SE_R} + \mathrm{SE_A} \tag{7}$$

Before starting the SE measurements, the setup was properly calibrated. A through-open-short-match (TOSM) calibration procedure was applied for each port using an 85521A OSLT Mechanical Calibration Kit.

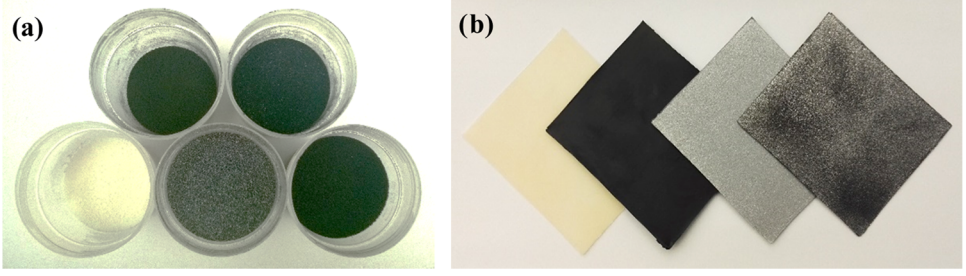

Figure 1. Visual aspect of some of the hybrid materials prepared: (a) empty and binary loaded microparticles containing metal and CNT fillers encapsulated in PA6 (DM samples); (b) molded composite plates obtained from the respective DM samples (from left to right): P-PA6, P-CNT5, P-Al5, DP-Al5-CNT5. The letter P stands for "composite plate" and DP stands for "dually loaded composite plate".

https://doi.org/10.1021/acsapm.2c00084
ACS Appl. Polym. Mater. 2022, 4, 3482−3490

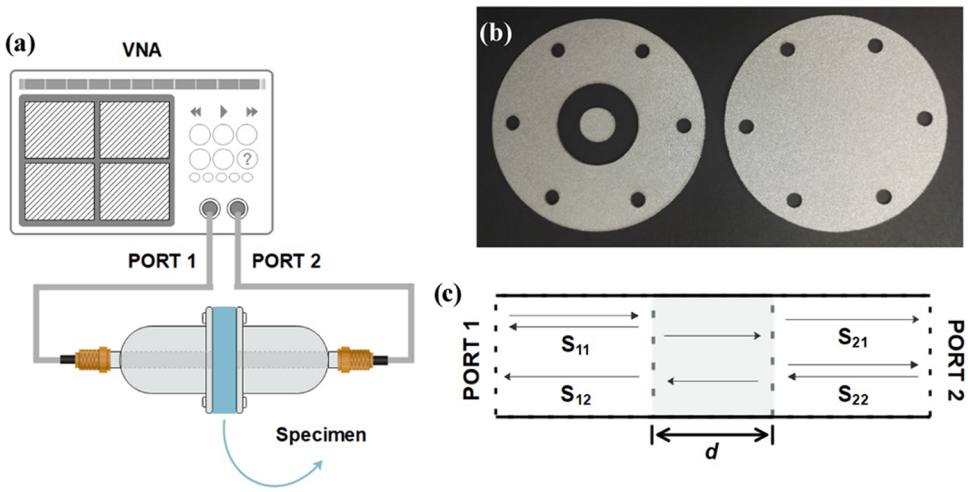

Figure 2. (a) Representation of the setup used for the EMI shielding measurements; (b) reference (left) and load (right) specimens of a molded sample plate; and (c) representation of the *S*-parameters through the coaxial transmission line (*d*, sample thickness).

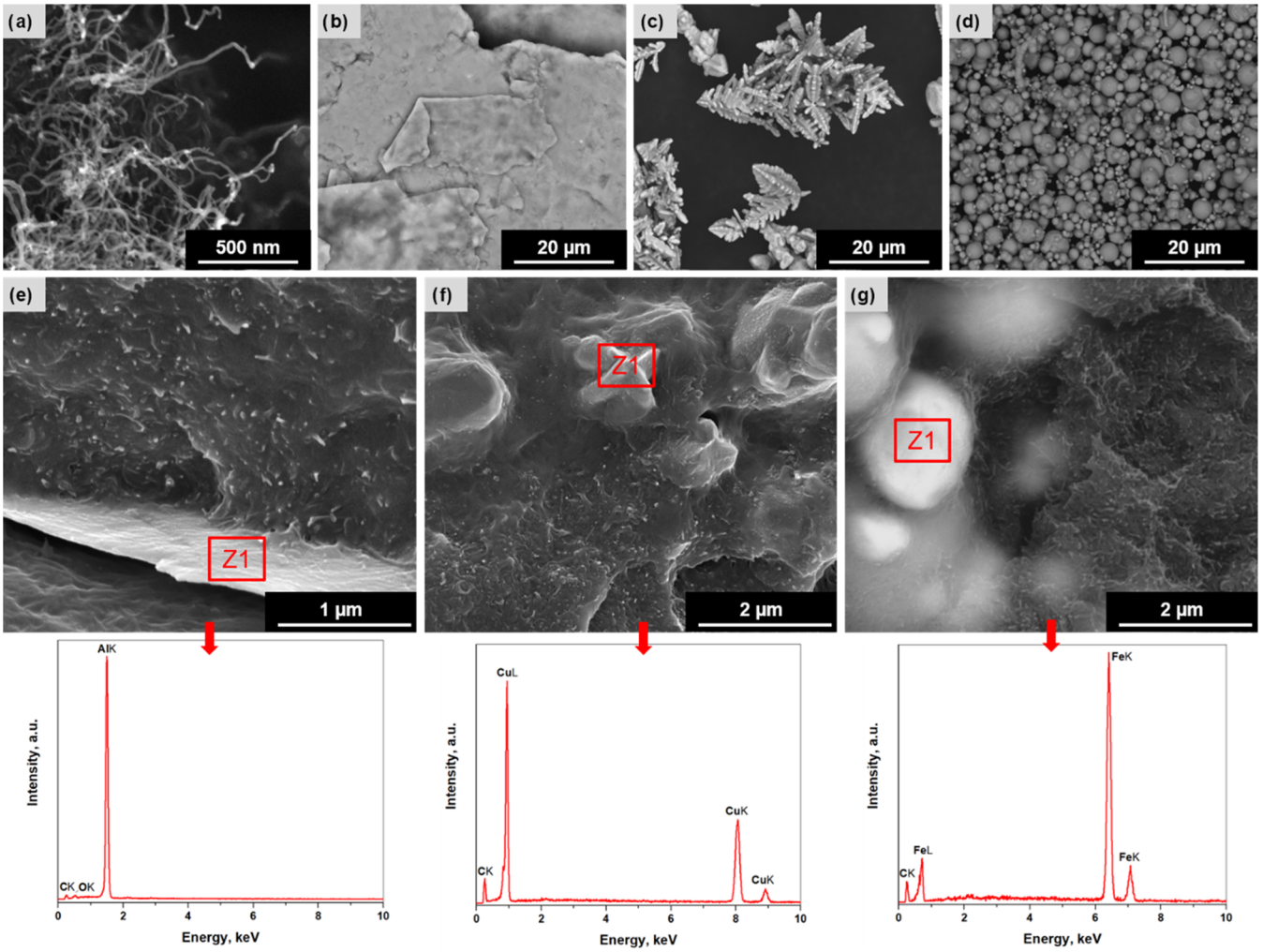

Figure 3. SEM micrographs of neat loads as received (a) CNT, (b) Al, (c) Cu, and (d) Fe, and of PA6 molded composites: (e) DP-Al5-CNT5, (f) DP-Cu5-CNT5, and (g) DP-Fe5-CNT5, with respective energy dispersive X-ray spectroscopy (EDS) analysis obtained in the site identified as Z1. In the sample designations, the letter P stands for composite plate, compression-molded from microparticles, and DP stands for plates molded from dually loaded microparticles.

https://doi.org/10.1021/acsapm.2c00084
ACS Appl. Polym. Mater. 2022, 4, 3482−3490

3. RESULTS AND DISCUSSION

3.1. Preparation and Initial Sample Characterization. All details about the synthesis, morphology, and crystalline structure of the selected MP precursors containing metal/carbonaceous loads obtained by AAROP in solution, as well as about the mechanical properties in tension and the electrical conductivity of the respective compression-molded PA6/metal or PA6/metal/CNT hybrids were communicated in previous works.[28,30] The focus of the present study is on the EMI shielding properties of selected compression-molded metal/CNT-loaded composite plates that were never studied before.

As seen in Table 1, the conversion of ECL to PA6 is 56% for empty MP and 42−63% for the samples with mono- or binary loads. In accordance with [28,30] this anionic polymerization process leads to the formation of PA6 MP with viscometric molecular weights around 33 kD. It should be noted that both filler types employed do not need any modification for better compatibilization with the matrix PA6. The reason why the MP yields are around 50−60% and not closing 98−99% as in the bulk AAROP is related to limited chain propagation due to the crystallization and precipitation of MP when AAROP is carried in solution.[30] The real load RL of the combined metal/CNT fillers determined by TGA was 2−7% higher than the 10 wt % calculated with respect to the ECL monomer that was fed into the AAROP. Apparently, the RL value will depend on the conversion of ECL to PA6 being higher at lower polymerization yields and vice-versa.

The thermal stability of metal/CNT-loaded microparticulate samples and the mechanical properties of the molded plates thereof were disclosed in our previous work.[30] The best thermal resistance was obtained with the PA6/Al/CNT and PA6/Fe/CNT sample displaying 10% weight losses at temperatures 65−70 °C higher than the neat PA6 reference. The mechanical properties in tension disclosed in the same ref 30 were the best with the PA6/Cu/CNT and PA6/Fe/CNT plates with tension at break σ_{br} = 57−60 MPa and elastic modulus E around 2 GPa, followed by the PA6-Al-CNT compositions with σ_{br} = 44−52 MPa and E = 1.6−2.6 GPa. Neat PA6 reference samples obtained in the same way showed σ_{br} = 60 MPa and E = 1.6 GPa. Based on this preliminary information on the thermal and mechanical behavior, the powders with metal/CNT compositions presented in Table 1 of this work were selected for further characterization.

3.2. Morphology of the Binary Composites. The morphology of the binary PA6 plates can be assessed from the SEM micrographs presented in Figure 3. Images (a)−(d) provide information about the size and shape of the particles in the neat CNT, Al, Cu, and Fe loads, respectively. As observed in Figure 3a, the CNT filler comprises 10−20 nm thick fibrils, tangled, and with considerable length. Regarding the metal payloads, the Al particles (Figure 3b) are shaped as platelets with maximum sizes of 80−100 μm and thicknesses below 15 μm. The Cu particles (Figure 3c) display complex dendritic shapes with sizes in the 20−40 μm range, and the Fe particles (Figure 3d) are spherical with diameters between 1 and 5 μm.

The morphological features after compression molding of MP to plates with binary CNT/metal load can be seen in micrographs (e)−(g). A good dispersion at the level of single CNT filaments is observed within the PA6 matrix, with almost no aggregation and also a good contact between the CNT and the respective metal particles. The EDS analysis of the PA6 binary composites identifies the emission peaks of Al, Cu, or Fe when the respective metal particles embedded in the PA6 matrix are hit.

3.3. Electrical Conductivity. The electrical conductivity values, σ_{dc}, measured by broadband dielectric spectroscopy of the binary metal/CNT composite plates (DP samples) are shown in Table 2. For comparison, the σ_{dc} values of the neat PA6 and molded composites containing only metal or CNT payloads (P-samples) are also presented.

Table 2. Electrical Conductivities of 1 mm Thick PA6-Based Composites Determined at T = 20 °C and f = 0.1 Hz[a]

sample	σ_{dc}, S/cm
P-PA6	4.77×10^{-14}
P-Al5	7.54×10^{-12}
P-Cu5	2.24×10^{-12}
P-Fe5	2.88×10^{-12}
P-CNT5	9.97×10^{-5}
DP-Al7-CNT3	1.42×10^{-5}
DP-Al5-CNT5	7.14×10^{-4}
DP-Al3-CNT7	6.61×10^{-3}
DP-Cu5-CNT5	2.78×10^{-3}
DP-Fe5-CNT5	4.04×10^{-4}

[a]In the sample designations, the letter P stands for composite plate, compression-molded from microparticles, and DP stands for plates molded from dually loaded microparticles.

As expected, the hybrids containing metal fillers only maintain the electrical insulating properties of the neat PA6 matrix, the σ_{dc} values being in the range of 10^{-12} S/cm. These results confirm previous conductivity measurements in similar PA6/metal hybrids containing 5−10 wt % of metal fillers.[28] Apparently, the percolation threshold in the latter was not achieved. Moreover, the Maxwell−Wagner−Sillars interfacial polarization theory predicts polarization and charge accumulation at the PA6/metal interfaces thus blocking the free movement of charges, i.e., electrical conduction.[34] On the other hand, the dispersion of CNT with 5 wt % resulted in a notable growth of σ_{dc} with 9 decades reaching values of semiconductor materials, meaning that the percolation threshold in relation to the CNT filler was achieved. Relating these results to the morphology of the CNT (Figure 3a), it can be inferred that the nanometric sections of the CNT entities and their homogeneous distribution within the PA6 matrix are important factors enhancing the electrical conductivity. The high aspect ratio of the CNT also contributes to the σ_{dc} increase, building a conductive network with effective charge transfer. According to Table 2, in the binary metal/CNT samples, even higher conductivities are achieved reaching values slightly above 10^{-3} S/cm for the DP-Al5-CNT5 and DP-Cu5-CNT5 samples. This is up to 2 orders of magnitude higher than in the P-CNT5 sample, i.e., the presence of Al and Cu along with CNT has a synergetic effect on the electrical conductivity. Most probably, this effect should be related to the improved charge transport in the DP samples.

3.4. EMI Shielding Performance. The total EMI shielding performance of the conductive binary PA6 composites in the form of plain films with two different thicknesses was evaluated within a frequency range of 3.0−12.4 GHz (Figure 4). This microwave range is widely used in communication applications such as telephones, microwaves, and television picture transmission. For comparison, PA6 composites with mono loads of CNT and neat PA6 were also

https://doi.org/10.1021/acsapm.2c00084
ACS Appl. Polym. Mater. 2022, 4, 3482−3490

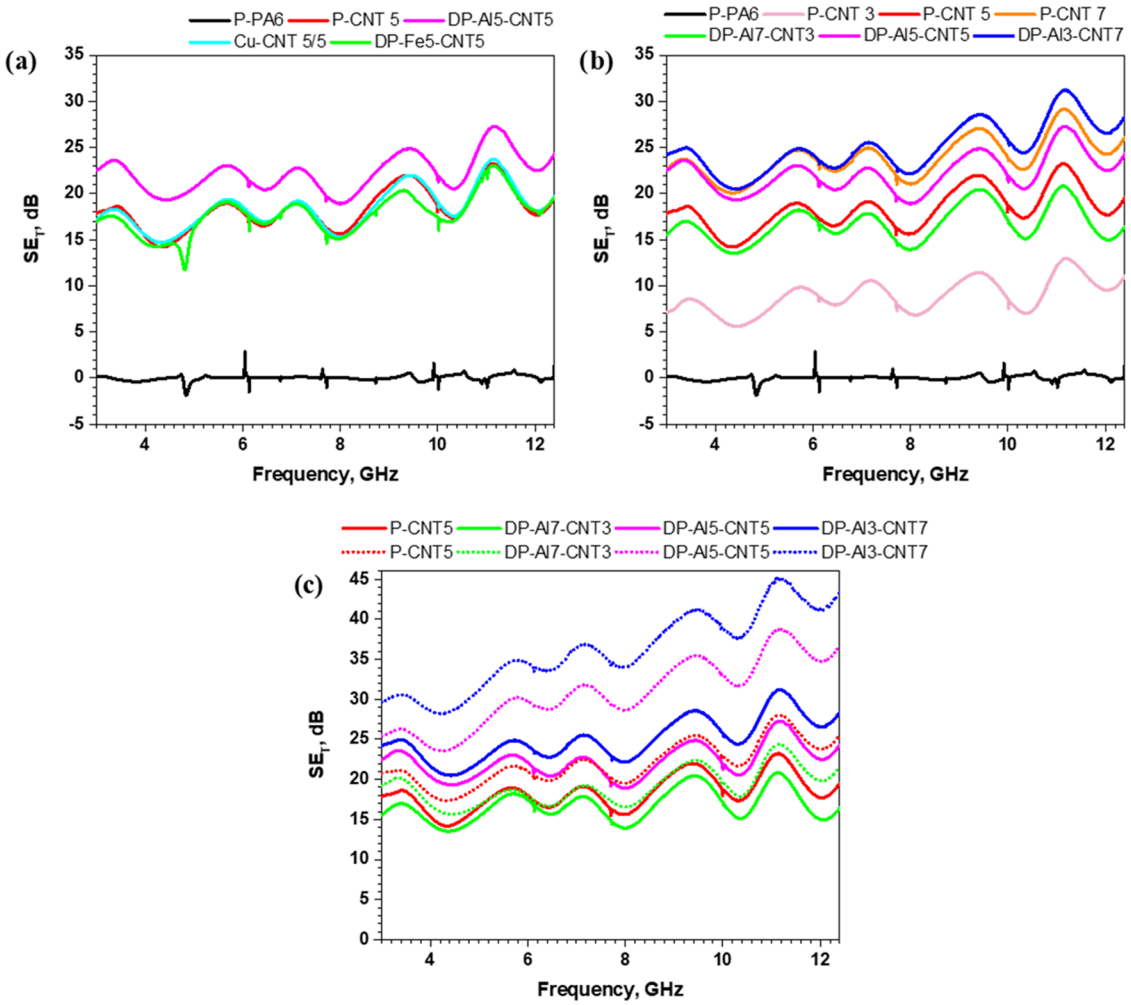

Figure 4. (a) SE_T of metal/CNT 5/5 wt % composites, (b) SE_T of Al/CNT composites with various compositions, and (c) comparison between SE_T of the 1- and 2 mm thick, binary Al/CNT hybrids; 1 mm thick composites are represented with solid lines, and dashed lines represent 2 mm composites. The results for neat PA6 and PA6/CNT hybrid plates are presented to enable comparison. For sample designations, see Table 2.

investigated. The SE_T plots of the 1 mm thick composite plates are presented in Figure 4a,b, and those with 2 mm thickness are in Figure 4c. Table S1 summarizes all numeric data from the SE measurements.

As expected, the neat PA6 is completely transparent for EM waves over the whole frequency range studied (Figure 4a, sample P-PA6) due to its insulator properties. In the presence of 5 wt % of CNT (Figure 4a, sample P-CNT5), a significant enhancement of the EMI shielding capability is achieved, with the SE_T values varying in the range of 18−22 dB. Notably, the presence of binary Al-CNT filler (the DP-Al5-CNT5 sample) additionally increases the SE_T above 25 dB at 12.4 GHz, i.e., a clear synergetic effect is observed. Such synergism was not found in samples DP-Cu5-CNT5 and DP-Fe5-CNT5, compared to the mono-loaded P-CNT5 sample. Generally, the EMI shielding performance of the DP samples is proportional to their σ_{dc} (Table 2) but another important factor is the volume percentage of the metal particles in the PA6 matrix, which is the highest in the case of Al-containing samples (Table 1). On the other hand, among all metal fillers employed, it is the Al that has the largest particle size in the form of platelets (Figure 3b). Hence, it can be inferred that besides the attenuation of the EM waves due to the conductive losses, some of the EM waves can be additionally reflected by the lamellar Al surfaces, thus reinforcing the EMI attenuation effect of the Al-containing samples.

Generally, all loaded samples in Figure 4 display a sinusoidal curve profile whose maxima slightly increase with frequency. This undulation can be due to reflection events becoming stronger at higher frequencies, while the absorption mechanism can explain the increased values. As shown in Table S1 and Figure S1, the contribution of the EM wave absorption component SE_A in SE_T is clearly predominant, i.e., absorption is the main EMI shielding mechanism in the studied samples. This is expected, having in mind the inversely proportional frequency dependence of SE_R. Since SE_T values in the range of 20−40 dB are considered good for many commercial applications,[4,35] our values between 19.6 dB (DP-Fe5-CNT5) and 24.3 dB (DP-Fe5-CNT5) for all DP samples with a metal/CNT content of 5/5 wt % at 1 mm thickness indicate good potential for the practice.

Among all binary reinforced samples, DP-Al5-CNT5 showed the best EMI shielding performance being, at the same time, the most cost-effective. Therefore, DP samples with dual Al-CNT loads with various compositions were selected for further studies of SE_T including variations of the Al/CNT proportion (Figure 4b), as well as increasing the sample thickness to 2 mm (Figure 4c). Figure S2 shows the frequency dependences of

https://doi.org/10.1021/acsapm.2c00084
ACS Appl. Polym. Mater. 2022, 4, 3482−3490

SE_R and SE_A, and all of the respective numeric data are summarized in Table S1. It can be seen that the presence of an Al/CNT load of 3/7 wt % has a synergetic effect upon the SE_T values only above 8 GHz, while at lower frequencies, P-CNT7 and DP-Al3-CNT7 perform similarly. Evidently, increasing the CNT content creates a denser conducting network with higher electrical conductivity leading to a more effective EM wave attenuation. At higher frequencies, additional dissipation of the mobile charge carriers occurs due to the presence of Al platelets. Thus, at 12.4 GHz, mono-loaded P-CNT samples display SE_T values between 11 dB (P-CNT3) and 26 dB (P-CNT7), while values close to 30 dB were reached for the DP-Al3-CNT7 sample (Figure 4b and Table S1).

The influence of thickness was also evaluated in further EMI shielding studied with the Al-CNT system. Selected composites with 2 mm of thickness were prepared and subjected to comparative EMI shielding tests at 3.0−12.4 GHz with 1 mm thick composite plates (Figure 4c). Figure S3 shows the plots for SE_A and SE_R contributions, and Table S2 summarizes all of the numeric data obtained at selected frequencies for the 2 mm thick composites. To quantify the improvements in the EMI shielding performance related to the influence of thickness, the improvement factor (IF) was determined for the SE_T values at 12.4 GHz, and the results are presented in Table 3.

Table 3. Comparison between EMI SE Data of the 1 and 2 mm Thick Selected PA6-Based Composites at 12.4 GHz

	SE_T, dB		
sample	1 mm	2 mm	IF, %[a] *With*
P-CNT5	19.56	25.54	30.57
DP-Al7-CNT3	16.45	21.66	31.67
DP-Al5-CNT5	24.33	36.71	50.88
DP-Al3-CNT7	28.40	43.51	53.20

[a] *With* respect to 1 mm thick molded sample. For sample designations, see Table 2.

According to the results obtained, the EMI efficiency increases significantly with the sample thickness, which was also expected having in mind the following dependences[36,37]

$$SE_A(dB) = 8.686d\sqrt{\pi f\sigma\mu} \quad (8)$$

$$SE_R(dB) = 39.5 + 10\log\frac{\sigma}{2\pi f\mu} \quad (9)$$

where d is the thickness, σ is the electrical conductivity, f is the frequency, and μ is the magnetic permeability.

Notably, SE_R is independent of the sample's thickness. For the 2 mm thick DP-Al3-CNT7 sample at a frequency of 12.4 GHz, the SE_T value reached 43.5 dB, representing an improvement factor IF of more than 53% with respect to a 1 mm thick sample with equivalent composition.

To better assess the EMI shielding potential of the binary composites of this study obtained via microencapsulation, a comparison with other thermoplastic composites obtained by other authors and by means of melt-mixing techniques is made in Table 4. It can be seen that the results of this study are close to or even better than the majority of the SE_T data presented. The only exception is the ABS-based composite with 15 wt % of CNT, i.e., 3 times more than in the present study. The excellent EMI shielding performance of our composites can be explained by the metal particles' contribution on one hand, and by the microencapsulation concept for the synthesis of thermoplastic composites applied in this work, on the other.

Using the microencapsulation concept enables the easy and rapid preparation of binary loaded, metal/CNT-containing microparticles that are easily transformed into molded plates with a high concentration of well-distributed metal and CNT fillers.

4. CONCLUSIONS

This work presents and discusses the first proof that PA6-based composite plates with good EMI shielding properties can be produced by reactive microencapsulation of binary metal/CNT fillers by means of AAROP of caprolactam in solution carried out in the presence of the fillers and subsequent compression molding of the resulting hybrid powders. By tuning the metal type and the metal/CNT composition, very good EMI shielding properties of the PA6-based composites were obtained reaching over 43 dB at 12.4 GHz and 2 mm thickness, applying Al and CNT at a weight ratio of 3/7 wt %. This result compares favorably with the existing thermoplastic EMI shielding materials. The conductivity of this sample was 6.6×10^{-3} S/cm, which is 11 orders of magnitude higher than the neat PA6 matrix, which is completely transparent for the EM waves. The excellent EMI shielding capability of the Al/CNT thermoplastic composites was attributed to the enhanced electrical conductivity due to the CNT fine dispersion and to the synergetic effect of the Al platelets that enhance the shielding properties above 8 GHz. The comparison between the SE_A and SE_R indicates absorption as the predominant shielding mechanism in all of the metal/CNT-filled PA6 composites. From a practical point of view, this is advantageous since secondary pollution by reflected electromagnetic waves is avoided. Moreover, the synthesis of binary loaded PA6 microparticles and their transformation by compression molding is practical, simple, versatile, and well adapted for scaling, which is important for commercial applications.

Table 4. EMI Shielding Properties of Thermoplastic Composites Loaded with CNT[a]

matrix polymer	CNT load, wt %	processing method	thickness, mm	maximum SE_T, dB	frequency range, GHz	ref
ABS	15	solution casting and compression molding	1.1	50	8.2−12.4	38
PE	5	mechanic mixture and compression molding	2.1	46.2	8.2−12.4	39
PTT	3	melt mixing and compression molding	2	38	2.65−3.95	40
PS	20	compression molding	2	30	8.2−12.4	41
ABS/PA6	3	masterbatch and injection molding	N/A	29	0.03−1.5	23
PC	2	solution casting and compression molding	5.6	23.1	8.2−12.4	42

[a] ABS = acrylonitrile-butadiene-styrene terpolymer; PE = polyethylene; PTT = poly(trimethylene terephthalate); PS = polystyrene; PC = bisphenol A polycarbonate.

https://doi.org/10.1021/acsapm.2c00084
ACS Appl. Polym. Mater. 2022, 4, 3482−3490

■ ASSOCIATED CONTENT

Supporting Information

The Supporting Information is available free of charge at https://pubs.acs.org/doi/10.1021/acsapm.2c00084.

Supporting plots on SE_A and SE_R contributions in PA6-based composites: metal/CNT = 5/5 wt %, Al/CNT with different compositions and 1 and 2 mm thick Al/CNT composites, and supporting tables with EMI shielding properties of PA6-based composites (PDF)

■ AUTHOR INFORMATION

Corresponding Author

Zlatan Z. Denchev − *Institute for Polymers and Composites (IPC), Universidade do Minho, 4800-058 Guimarães, Portugal;* orcid.org/0000-0002-9057-9380; Email: denchev@dep.uminho.pt

Authors

Filipa M. Oliveira − *Institute for Polymers and Composites (IPC), Universidade do Minho, 4800-058 Guimarães, Portugal;* Present Address: Department of Inorganic Chemistry, Faculty of Chemical Technology, University of Chemistry and Technology Prague, Technická 5, 166 28 Prague 6, Czech Republic

Luís Martins − *Institute for Polymers and Composites (IPC), Universidade do Minho, 4800-058 Guimarães, Portugal*

Nadya V. Dencheva − *Institute for Polymers and Composites (IPC), Universidade do Minho, 4800-058 Guimarães, Portugal*

Tiberio A. Ezquerra − *Instituto de Estructura de la Materia, IEM-CSIC, 28006 Madrid, Spain*

Complete contact information is available at: https://pubs.acs.org/10.1021/acsapm.2c00084

Author Contributions

This manuscript was written through the contributions of all authors. All authors have approved the final version of the manuscript.

Notes

The authors declare no competing financial interest.

■ ACKNOWLEDGMENTS

The authors gratefully acknowledge the technical support of Hugo Mostardinha from the Instituto de Telecomunicações—Aveiro during the EMI shielding measurements and the financial support of Fundação para a Ciência e Tecnologia (FCT), Project UID/CTM/50025/2019. F.M.O. thanks FCT for the Ph.D. grant PD/BD/114372/2016 (AdvaMTech—Ph.D. Program in Advanced Materials and Processing). The assistance of Prof. Nuno Carvalho from the University of Aveiro, Portugal, in the EMI shielding experiments is also gratefully acknowledged.

■ ABBREVIATIONS

AAROP, activated anionic ring-opening polymerization; *A*, absorption; A_{eff}, effective absorption; CNT, carbon nanotubes; CPC, conductive polymer composites; DM samples, hybrid powders of PA6 containing binary metal/CNT fillers; DP-samples, composite plates obtained by compression molding of DM samples; ECL, ε-caprolactam; EM, electromagnetic; EMI, electromagnetic interference; EMI SE, electromagnetic interference shielding effectiveness; *M*, multiple reflections; M-samples, hybrid powders of PA6 containing single Me or CNT filler; P-samples, composite plates obtained by compression molding of M-samples; PA6, polyamide 6; *R*, reflection; SE, shielding effectiveness; SE_A, shielding effectiveness by absorption; SE_M, shielding effectiveness by multiple reflections; SE_R, shielding effectiveness by reflection; SE_T, total EMI SE

■ REFERENCES

(1) Li, T.-T.; Chen, A.-P.; Hwang, P.-W.; Pan, Y.-J.; Hsing, W.-H.; Lou, C.-W.; Chen, Y.-S.; Lin, J.-H. Synergistic Effects of Micro-/Nano-Fillers on Conductive and Electromagnetic Shielding Properties of Polypropylene Nanocomposites. *Mater. Manuf. Processes* **2018**, *33*, 149−155.

(2) Erogul, O.; Oztas, E.; Yildirim, I.; Kir, T.; Aydur, E.; Komesli, G.; Irkilata, H. C.; Irmak, M. K.; Peker, A. F. Effects of Electromagnetic Radiation from a Cellular Phone on Human Sperm Motility: An In Vitro Study. *Arch. Med. Res.* **2006**, *37*, 840−843.

(3) Chung, D. D. L. Electromagnetic Interference Shielding Effectiveness of Carbon Materials. *Carbon* **2001**, *39*, 279−285.

(4) Thomassin, J.-M.; Jérôme, C.; Pardoen, T.; Bailly, C.; Huynen, I.; Detrembleur, C. Polymer/Carbon Based Composites as Electromagnetic Interference (EMI) Shielding Materials. *Mater. Sci. Eng. R* **2013**, *74*, 211−232.

(5) Abbasi, H.; Antunes, M.; Velasco, J. I. Recent Advances in Carbon-Based Polymer Nanocomposites for Electromagnetic Interference Shielding. *Prog. Mater. Sci.* **2019**, *103*, 319−373.

(6) Al-Saleh, M. H.; Sundararaj, U. A Review of Vapor Grown Carbon Nanofiber/Polymer Conductive Composites. *Carbon* **2009**, *47*, 2−22.

(7) Cai, J.; Wang, L.; Duan, H.; Zhang, Y.; Wang, X.; Wan, G.; Zhong, Z. Porous Polyamide 6/Carbon Black Composite as an Effective Electromagnetic Interference Shield. *Polym. Int.* **2022**, *71*, 247−254.

(8) Biswas, S.; Arief, I.; Panja, S. S.; Bose, S. Absorption-Dominated Electromagnetic Wave Suppressor Derived from Ferrite-Doped Cross-Linked Graphene Framework and Conducting Carbon. *ACS Appl. Mater. Interfaces* **2017**, *9*, 3030−3039.

(9) Mohan, R. R.; Varma, S. J.; Faisal, M.; S, J. Polyaniline/Graphene Hybrid Film as an Effective Broadband Electromagnetic Shield. *RSC Adv.* **2015**, *5*, 5917−5923.

(10) Chen, Y.; Li, Y.; Yip, M.; Tai, N. Electromagnetic Interference Shielding Efficiency of Polyaniline Composites Filled with Graphene Decorated with Metallic Nanoparticles. *Compos. Sci. Technol.* **2013**, *80*, 80−86.

(11) Singh, A. K.; Shishkin, A.; Koppel, T.; Gupta, N. A Review of Porous Lightweight Composite Materials for Electromagnetic Interference Shielding. *Composites, Part B* **2018**, *149*, 188−197.

(12) Sankaran, S.; Deshmukh, K.; Ahamed, M. B.; Pasha, S. K. K. Recent Advances in Electromagnetic Interference Shielding Properties of Metal and Carbon Filler Reinforced Flexible Polymer Composites: A Review. *Composites, Part A* **2018**, *114*, 49−71.

(13) Koo, C. M.; Shahzad, F.; Kumar, P.; Yu, S.; Lee, S. H.; Hong, J. P. Polymer-Based EMI Shielding Materials. In *Advanced Materials for Electromagnetic Shielding: Fundamentals, Properties, and Applications*; Jaroszewski, M.; Thomas, S.; Rane, A. V., Eds.; John Wiley & Sons, Inc., 2019; pp 177−217.

(14) Jiang, D.; Murugadoss, V.; Wang, Y.; Lin, J.; Ding, T.; Wang, Z.; Shao, Q.; Wang, C.; Liu, H.; Lu, N.; et al. Electromagnetic Interference Shielding Polymers and Nanocomposites - A Review. *Polym. Rev.* **2019**, *59*, 280−337.

(15) Dhakate, S. R.; Subhedar, K. M.; Singh, B. P. Polymer Nanocomposite Foam Filled with Carbon Nanomaterials as an Efficient Electromagnetic Interference Shielding Material. *RSC Adv.* **2015**, *5*, 43036−43057.

(16) Ganguly, S.; Bhawal, P.; Ravindren, R.; Das, N. C. Polymer Nanocomposites for Electromagnetic Interference Shielding: A Review. *J. Nanosci. Nanotechnol.* **2018**, *18*, 7641−7669.

(17) Ghosh, S. K.; Das, T. K.; Ghosh, S.; Remanan, S.; Nath, K.; Das, P.; Das, N. C. Selective Distribution of Conductive Carbonaceous Inclusion in Thermoplastic Elastomer: A Wet Chemical Approach of Promoting Dual Percolation and Inhibiting Radiation Pollution in X-Band. *Compos. Sci. Technol.* **2021**, *210*, No. 108800.
(18) Ganguly, S.; Ghosh, S.; Das, P.; Das, T. K.; Ghosh, S. K.; Das, N. C. Poly(N-Vinylpyrrolidone)-Stabilized Colloidal Graphene-Reinforced Poly(Ethylene-Co-Methyl Acrylate) to Mitigate Electromagnetic Radiation Pollution. *Polym. Bull.* **2020**, *77*, 2923−2943.
(19) Xu, H.; Li, Y.; Han, X.; Cai, H.; Gao, F. Carbon Black Enhanced Wood-Plastic Composites for High-Performance Electromagnetic Interference Shielding. *Mater. Lett.* **2021**, *285*, No. 129077.
(20) Duan, H.; Zhu, H.; Yang, Y.; Hou, T.; Zhao, G.; Liu, Y. Facile and Economical Fabrication of Conductive Polyamide 6 Composites with Segregated Expanded Graphite Networks for Efficient Electromagnetic Interference Shielding. *J. Mater. Sci.: Mater. Electron.* **2018**, *29*, 1058−1064.
(21) Yoo, T. W.; Lee, Y. K.; Lim, S. J.; Yoon, H. G.; Kim, W. N. Effects of Hybrid Fillers on the Electromagnetic Interference Shielding Effectiveness of Polyamide 6/Conductive Filler Composites. *J. Mater. Sci.* **2014**, *49*, 1701−1708.
(22) Lee, K. P. M.; Baum, T.; Shanks, R.; Daver, F. Graphene−Polyamide-6 Composite for Additive Manufacture of Multifunctional Electromagnetic Interference Shielding Components. *J. Appl. Polym. Sci.* **2021**, *138*, No. 49909.
(23) Jang, J.; Lee, H. S.; Kim, J. W.; Kim, S. Y.; Kim, S. H.; Hwang, I.; Kang, B. J.; Kang, M. K. Facile and Cost-Effective Strategy for Fabrication of Polyamide 6 Wrapped Multi-Walled Carbon Nanotube via Anionic Melt Polymerization of ε-Caprolactam. *Chem. Eng. J.* **2019**, *373*, 251−258.
(24) Schaefer, D. W.; Justice, R. S. How Nano Are Nano-Composites? *Macromolecules* **2007**, *40*, 8501−8517.
(25) Ojijo, V.; Ray, S. S. Processing Strategies in Bionanocomposites. *Prog. Polym. Sci.* **2013**, *38*, 1543−1589.
(26) Schadler, L. S. Polymer-Based and Polymer-Filled Nanocomposites. In *Nanocomposite Science and Technology*; Ajayan, M.; Schadler, L. S.; Braun, P. V., Eds.; Wiley-VCH Verlag GmbH & Co. KGaA: Weinheim, 2003; pp 77−153.
(27) Dencheva, N.; Denchev, Z.; Lanceros-Méndez, S.; Ezquerra Sanz, T. One-Step in Situ Synthesis of Polyamide Microcapsules with Inorganic Payload and Their Transformation into Responsive Thermoplastic Composite Materials. *Macromol. Mater. Eng.* **2016**, *301*, 119−124.
(28) Brêda, C.; Dencheva, N.; Lanceros-Mendez, S.; Denchev, Z. Preparation and Properties of Metal-Containing Polyamide Hybrid Composites via Reactive Microencapsulation. *J. Mater. Sci.* **2016**, *51*, 10534−10554.
(29) Oliveira, F.; Dencheva, N.; Martins, P.; Lanceros-Mendez, S.; Denchev, Z. Reactive Microencapsulation of Carbon Allotropes in Polyamide Shell-Core Structures and Their Transformation in Hybrid Composites with Tailored Electrical Properties. *eXPRESS Polym. Lett.* **2016**, *10*, 160−175.
(30) Oliveira, F.; Dencheva, N.; Lanceros-Méndez, S.; Nunes, T. G.; Denchev, Z. Binary Polyamide Hybrid Composites Containing Carbon Allotropes and Metal Particles with Radiofrequency Shielding Effect. *Polym. Compos.* **2019**, *40*, E1338−E1352.
(31) Kremer, F.; Schönhals, A. *Broadband Dielectric Spectroscopy*, 1st ed.; In Kremer, F.; Schönhals, A., Eds.; Springer-Verlag: Berlin, 2003.
(32) Linares, A.; Canalda, J. C.; Cagiao, M. E.; García-Gutiérrez, M. C.; Nogales, A.; Martín-Gullón, I.; Vera, J.; Ezquerra, T. A. Broad-Band Electrical Conductivity of High Density Polyethylene Nanocomposites with Carbon Nanoadditives: Multiwall Carbon Nanotubes and Carbon Nanofibers. *Macromolecules* **2008**, *41*, 7090−7097.
(33) Ezquerra, T. A.; Canalda, J. C.; Sanz, A.; Linares, A. On the Electrical Conductivity of PVDF Composites with Different Carbon-Based Nanoadditives. *Colloid Polym. Sci.* **2014**, *292*, 1989−1998.
(34) Steeman, P. A. M.; van Turnhout, J. Dielectric Properties of Inhomogeneous Media. In *Broadband Dielectric Spectroscopy*; Kremer, F.; Schönhals, A., Eds.; Springer: Berlin, 2003; pp 495−522.
(35) Yan, D.-X. X.; Pang, H.; Li, B.; Vajtai, R.; Xu, L.; Ren, P.-G. G.; Wang, J.-H. H.; Li, Z.-M. M. Structured Reduced Graphene Oxide/Polymer Composites for Ultra-Efficient Electromagnetic Interference Shielding. *Adv. Funct. Mater.* **2015**, *25*, 559−566.
(36) Al-Saleh, M. H.; Sundararaj, U. Electromagnetic Interference Shielding Mechanisms of CNT/Polymer Composites. *Carbon* **2009**, *47*, 1738−1746.
(37) Gooch, J. W.; Daher, J. K. Fundamentals of Electromagnetic Shielding. In *Electromagnetic Shielding and Corrosion Protection for Aerospace Vehicles*; Springer: New York, NY, 2007; pp 17−24.
(38) Al-Saleh, M. H.; Saadeh, W. H.; Sundararaj, U. EMI Shielding Effectiveness of Carbon Based Nanostructured Polymeric Materials: A Comparative Study. *Carbon* **2013**, *60*, 146−156.
(39) Jia, L.-C.; Yan, D.-X.; Cui, C.-H.; Jiang, X.; Ji, X.; Li, Z.-M. Electrically Conductive and Electromagnetic Interference Shielding of Polyethylene Composites with Devisable Carbon Nanotube Networks. *J. Mater. Chem. C* **2015**, *3*, 9369−9378.
(40) Kunjappan, A. M.; Poothanari, M. A.; Ramachandran, A. A.; Padmanabhan, M.; Mathew, L.; Thomas, S. High-Performance Electromagnetic Interference Shielding Material Based on an Effective Mixing Protocol. *Polym. Int.* **2019**, *68*, 637−647.
(41) Arjmand, M.; Apperley, T.; Okoniewski, M.; Sundararaj, U. Comparative Study of Electromagnetic Interference Shielding Properties of Injection Molded versus Compression Molded Multi-Walled Carbon Nanotube/Polystyrene Composites. *Carbon* **2012**, *50*, 5126−5134.
(42) Maiti, S.; Suin, S.; Shrivastava, N. K.; Khatua, B. B. A Strategy to Achieve High Electromagnetic Interference Shielding and Ultra Low Percolation in Multiwall Carbon Nanotube−Polycarbonate Composites through Selective Localization of Carbon Nanotubes. *RSC Adv.* **2014**, *4*, 7979−7990.

https://doi.org/10.1021/acsapm.2c00084
ACS Appl. Polym. Mater. 2022, 4, 3482−3490